IEEE Access
Multidisciplinary ⋮ Rapid Review ⋮ Open Access Journal

Received July 2, 2020, accepted July 6, 2020, date of publication July 9, 2020, date of current version July 22, 2020.

Digital Object Identifier 10.1109/ACCESS.2020.3008158

Ultra-Local Model-Free Predictive Current Control Based on Nonlinear Disturbance Compensation for Permanent Magnet Synchronous Motor

LINGLIANG XU, GUIMING CHEN, AND QIAOYANG LI
College of Combat Support, Rocket Force University of Engineering, Xi'an 710025, China

Corresponding author: Lingliang Xu (lingliangxu@hotmail.com)

This work was supported in part by the National Natural Science Foundation of China under Grant 71601180.

ABSTRACT During motor operation, the motor parameters change, which causes parameter drift. They are also affected by internal and external unknown disturbances, which lead to reduced motor control performance, poor anti-interference performance, and low robustness. A method termed ultra-local model-free predictive current control (MFPCC) has previously been proposed to solve this problem; it uses only the input and output of the system and does not involve any motor parameters, because of which it is free of problems caused by model mismatch. However, the conventional MFPCC method requires adjustment of several control parameters and the estimated value of the total disturbance of the system has a certain deviation and a large pulsation, which result in obvious chattering of the motor output, low stability, reduced anti-interference performance, and low robustness. Therefore, this paper proposes an MFPCC method based on nonlinear disturbance compensation (NDC). This method does not involve any motor parameters, and it can more accurately and stably estimate the total system disturbance, and feedforward compensation, real-time update control information, only need to adjust two control parameters, the workload is small. Simulation results show that the proposed control method has high anti-interference performance, high robustness, small output ripple, and improved dynamic characteristics and that it can estimate the system disturbance accurately and stably.

INDEX TERMS Permanent magnet synchronous motor (PMSM), ultra-local, model-free predictive current control (MFPCC), current limiting, nonlinear disturbance compensation (NDC).

I. INTRODUCTION

A PMSM is a complex object with multiple variables, strong coupling, nonlinearity, and variable parameters; therefore, a reasonable control method needs to be adopted to improve its operating efficiency [1]–[4]. Conventional control methods include vector control and direct torque control (DTC). The vector control technology draws on the direct current (DC) motor control method to realize the current decoupling through coordinate transformation, and thus the decoupling of the magnetic field and torque. However, the vector control method cannot meet practical requirements when the motor is subjected to external disturbances or internal changes in parameters [5]–[8]. DTC abandons the decoupling concept of vector control and does not require coordinate transformation; this weakens the system's dependence on motor parameters. However, the inverter switch is not constant, which leads to large flux linkage and torque ripple [9]–[12]. Approaches such as sliding mode control, proportional resonance control, and the model predictive control (MPC) have been proposed for improving the PMSM control performance and solving problems such as the dependence and disturbance of the control model on the motor model and the parameter insensitivity [13], [14].

MPC is widely used because of its simple design and superior control performance. MPC uses the mathematical model of the control object to discretely obtain the predicted value and then optimizes the cost function to make the predicted value approach the expected value along the reference trajectory [15], [16]. MPC is classified into two types depending on the control variables: model predictive current control (MPCC) and model predictive torque control.

The associate editor coordinating the review of this manuscript and approving it for publication was Shihong Ding.

The MPCC performance depends on the accuracy of the parameters of the control object [17]. However, during the operation of a motor, its parameters are affected by factors such as temperature, magnetic field saturation, and operating state, which leads to parameter drift and model mismatch as well as a decrease in the control accuracy and degradation of the control performance.

Several solutions to this problem of MPCC performance degradation due to model mismatch have been proposed. A previous study [18] proposed a predictive function control method by simplifying the PMSM mathematical model in order to make the predicted value approach the actual value along the reference trajectory. An extended state observer (ESO) was designed to handle parameter changes, measurement interference, and external interference, and the observed interference terms were used as feedforward compensation. Another study [19] suggested that the accuracy of MPC is greatly affected by the sampling time and therefore proposed a generalized predictive control method based on a continuous-time predictive model. Aiming at the disturbance caused by the parameter change, a sliding mode disturbance compensator is designed to perform feedforward compensation. As a result, the actual output of the system contained two parts: the generalized predictive control output and the output of the synovial disturbance compensation. Literature [17] research revealed that the accuracy of the inductance and flux linkage parameters has a strong influence on the prediction accuracy; therefore, an incremental prediction model was first used to eliminate the influence of the flux linkage parameters. Then, an inductance jammer was designed to eliminate the influence of the inductance parameters, and the inductance value was extracted and updated in real time. This approach effectively reduced the sensitivity of the prediction model to parameters. One study [20] abandoned the conventional cost function and selected the best control vector on the basis of the current trajectory circle. The results revealed that this method has a simple design and can effectively reduce torque ripple and current ripple and improve the sensitivity of the control model.

A model-free control method uses only the input and output of the system without considering the influence of any parameters; in this case, known terms with parameters and unknown interference terms constitute the total interference terms of the system. As a result, the method prevents parameter drift from influencing the control model, improves the robustness of the control model, and reduces the parameter dependence of the control model [21], [22]. Because of its excellent control performance and simple design, this method is widely used in various fields [23]. A previous study [24] used a model-free control method that considered the interference caused by parameter changes, inverter nonlinearity, and cross-coupling terms in order to establish an ultra-local model. Parameter identification method was used to estimate the interference terms. The findings of the study showed that the developed model reduced current ripple to a certain extent and improved the dynamic response of the system. However, the pulsation of the estimated interference terms was large and the estimation accuracy of the method was low. Another study [25] investigated the effects of different sampling frequencies on MFPCC and reported that the system control accuracy may be reduced at lower sampling frequencies. In addition, an ESO was established to estimate the system disturbance. The results revealed that the method showed better performance in terms of the tracking error, current harmonics, and dynamic overshoot. However, a PMSM control system contains both matching disturbances, e.g., electromagnetic parameter changes, and nonmatching disturbances, e.g., external loads and mechanical parameter changes. The above-discussed disturbance compensation methods have certain limitations [26]. A study [27] proposed an ultra-local model and a deadbeat predictive control method. The model was established using the input and output variables of the speed loop, and the results showed that the method had high robustness and anti-interference performance.

With the aim of improving both the anti-interference performance of the PMSM system and its robustness to parameter changes, internal interference, and external interference, this paper proposes an ultra-local model-free predictive current control method based on nonlinear disturbance compensation (hereafter referred to as MFPCC + NDC method). This method uses only the system output and input and does not consider any parameter effects, and it is used to establish an ultra-local MFPCC model. Known matching terms containing parameter disturbances and unknown nonmatching terms constitute the total interference terms of the system. A nonlinear disturbance observer aimed at estimating the total interference terms is established, and it monitors the system disturbance and obtains accurate total interference items and updates the control system information in real time [28]–[30]. Simulation results reveal that the proposed method has small output ripple, small pulsation, high robustness, and high anti-interference performance under the condition of external interference and variable parameters and that it estimates the total interference terms more accurately and stably than conventional control methods. The main contributions of the paper are as follows.

1. For the PMSM model mismatch caused by motor parameter drift and system disturbance, this paper established the MFPCC method, which reduces the dependence on the PMSM model parameters and reduces the impact of control performance degradation caused by parameter changes and system disturbances.

2. The traditional MFPCC method has a large pulsation in the estimation of the total disturbance of the system, the accuracy of the estimated value is not high, and involves more parameters and a larger workload. PMSM is a non-linear complex system, so this paper proposes the NDC method, online estimation of the total system disturbance, and feed-forward compensation, real-time update control information, only need to determine two parameters, the workload is reduced.

3. A larger current will produce a larger electromagnetic torque, and the motor will be impacted, which is not conducive to the smooth operation of the motor. In order to prevent the generation of large current, the current limit control is established to improve the motor control performance.

The rest of the paper is structured as follows. Section II first introduces the principle of the ultra-local model and then derives an expression for ultra-local MFPCC of the PMSM system. Then, the section presents the construction of a nonlinear disturbance observer for monitoring the total disturbance of the system and performing feedforward compensation; it next describes the subsequent application of the forward-time Euler discrete method to obtain the reference voltage. Section III presents the design of a current-limiting link aimed at controlling the current output size. Section IV presents an analysis of the simulation results, and Section V summarizes the paper.

II. ESTABLISHMENT OF ULTRA-LOCAL MFPCC MODEL FOR PMSM

A. CONSTRUCTION OF ULTRA-LOCAL MODEL

The conventional ultra-local mathematical model is expressed as [23]

$$\dot{y} = F + \alpha u \tag{1}$$

Here, y is the system output, u is the system input, F is the sum of known and unknown interferences of the system, and α is a nonphysical scale factor of the designed model.

$$u = \frac{\dot{y}^* - \hat{F} + \xi}{\alpha} \tag{2}$$

Here, y^* is the expected output of the system, $\hat{F}$ is the estimated value of F, and ξ denotes the output of the designed controller.

$$\dot{e} + \xi = 0 \tag{3}$$

Here, $e = y^*$ - y, which denotes the tracking error. When a proportional-integral (PI) controller is used, equation (2) is rewritten as

$$u = \frac{\dot{y}^* - \hat{F} + K_p e}{\alpha} \tag{4}$$

$$\dot{e} + K_p e = 0 \tag{5}$$

where K_p is the proportional gain.

B. PMSM-BASED ULTRA-LOCAL MFPCC

The PMSM mathematical model is

$$\begin{cases} u_d = R_0 i_d + \dfrac{d\psi_d}{dt} - \omega_e \psi_q \\ u_q = R_0 i_q + \dfrac{d\psi_q}{dt} + \omega_e \psi_d \end{cases} \tag{6}$$

$$\begin{cases} \psi_d = L_d i_d + \psi_{f0} \\ \psi_q = L_q i_q \end{cases} \tag{7}$$

Here, u_d and u_q are the dq-axis voltage vectors, i_d and i_q are the dq-axis current vectors, ψ_d and ψ_q are the dq-axis components of the stator flux linkage, R_0 is the stator resistance, and L_d and L_q are the dq-axis inductances. For a surface-mounted PMSM, the stator inductance satisfies $L_d = L_q = L_0$. In the above equations, Ψ_{f0} is the permanent-magnet flux linkage, ω_e is the electrical angular velocity of the motor.

$$\begin{cases} u_d = R_0 i_d + L_d \dfrac{di_d}{dt} - \omega_e L_q i_q \\ u_q = R_0 i_q + L_q \dfrac{di_q}{dt} + \omega_e L_d i_d + \omega_e \psi_{f0} \end{cases} \tag{8}$$

Under consideration of parameter changes and unknown interference terms, equation (8) can be rewritten as

$$\begin{cases} u_d = (R_0 + \Delta R) i_d + (L_0 + \Delta L)\dfrac{di_d}{dt} \\ \qquad -\omega_e (L_0 + \Delta L) i_q + f_d \\ u_q = (R_0 + \Delta R) i_q + (L_0 + \Delta L)\dfrac{di_q}{dt} \\ \qquad +\omega_e (L_0 + \Delta L) i_d + \omega(\psi_{f0} + \Delta\psi_f) + f_q \end{cases} \tag{9}$$

Here, R_0, L_0, and Ψ_{f0} are the calibration values on the motor nameplate; ΔR, ΔL, and $\Delta\Psi_f$ are the parameter change values; and f_d and f_q are the unknown interference terms in the d-axis and q-axis, respectively. Equation (9) can be expressed as

$$\begin{cases} \dfrac{di_d}{dt} = \dfrac{u_d}{L_0} + (-\dfrac{\Delta L}{L_0}\dfrac{di_d}{dt} - \dfrac{(R_0 + \Delta R) i_d}{L_0} \\ \qquad + \dfrac{\omega_e (L_0 + \Delta L) i_q}{L_0} - \dfrac{f_d}{L_0}) \\ \dfrac{di_q}{dt} = \dfrac{u_q}{L_0} + (-\dfrac{\Delta L}{L_0}\dfrac{di_q}{dt} - \dfrac{(R_0 + \Delta R) i_q}{L_0} \\ \qquad - \dfrac{\omega_e (L_0 + \Delta L) i_d}{L_0} - \dfrac{\omega_e (\psi_{f0} + \Delta\psi_f)}{L_0} - \dfrac{f_q}{L_0}) \end{cases} \tag{10}$$

If we consider the dq-axis current as the system output, the dq-axis voltage as the system input, and the remaining terms as the sum of the known and unknown interference terms of the system, the ultra-local model-free control of the PMSM can be expressed as

$$\begin{cases} \dfrac{di_d}{dt} = \alpha_d u_d + F_d \\ \dfrac{di_q}{dt} = \alpha_q u_q + F_q \end{cases} \tag{11}$$

Here, α_d and α_q are the controller gains in the d-axis and q-axis, respectively.

$$\begin{cases} F_d = -\dfrac{\Delta L}{L_0}\dfrac{di_d}{dt} - \dfrac{(R_0 + \Delta R) i_d}{L_0} + \dfrac{\omega_e (L_0 + \Delta L) i_q}{L_0} \\ \qquad -\dfrac{f_d}{L_0} \\ F_q = -\dfrac{\Delta L}{L_0}\dfrac{di_q}{dt} - \dfrac{(R_0 + \Delta R) i_q}{L_0} + \dfrac{\omega_e (L_0 + \Delta L) i_d}{L_0} \\ \qquad + \dfrac{\omega_e (\psi_{f0} + \Delta\psi_f)}{L_0} - \dfrac{f_q}{L_0} \end{cases} \tag{12}$$

C. NDC

To improve both the robustness and anti-interference performance of the control model, the total disturbance of the system is estimated more accurately and updated in real time. A nonlinear disturbance observer is designed to estimate the total disturbance of the system for feedforward compensation. For PMSM based ultra-local model-free control expressed in equation (11), the nonlinear disturbance observer is designed as follows [31]:

$$\begin{cases} \dot{Z} = -l(x)Z - l(x)\{\lambda(x) + \alpha u\} \\ \hat{F} = Z + \lambda(x) \end{cases} \tag{13}$$

Here, $Z = [Z_d, Z_q]^{\mathrm{T}}$ is the internal state variable of the system, $l(x) = \begin{bmatrix} l_d(x) & 0 \\ 0 & l_q(x) \end{bmatrix}$ is the gain of the nonlinear disturbance observer, $\lambda(x) = [\lambda_d(x), \lambda_q(x)]^{\mathrm{T}}$ is the nonlinear function of the observer to be designed, $\alpha = \begin{bmatrix} \alpha_d & 0 \\ 0 & \alpha_q \end{bmatrix}$ is the dq-axis controller gain, $u = [u_d, u_q]^{\mathrm{T}}$ is the system input, and $\hat{F} = \left[\hat{F}_d, \hat{F}_q\right]^{\mathrm{T}}$ is the estimated value of the total disturbance.

The relationship between the observer gain and the nonlinear function to be designed is given as

$$l(x) = \frac{\partial \lambda(x)}{\partial x} \tag{14}$$

Define the total disturbance error e of the system as

$$e = F - \hat{F} \tag{15}$$

Then

$$\dot{e} = \dot{F} - \dot{\hat{F}} = \dot{F} - \left[\dot{Z} + \dot{\lambda}(x)\right] = -l(x)e + \dot{F} \tag{16}$$

Use the Lyapunov function to verify the stability of the NDC controller and define the function V

$$V = \frac{1}{2}e^2 \tag{17}$$

Considering that the total disturbance F and $\dot{F}$ are bounded, which is $\lim_{t\to\infty} \dot{F} = 0$. Differentiate the equation (17) to get

$$\dot{V} = e\dot{e} = e \times \left[-l(x)e + \dot{F}\right] = -l(x)e^2 \leq 0 \tag{18}$$

According to the principle of Lyapunov function stability, the NDC system is progressively stable.

D. REFERENCE VOLTAGE CALCULATION

The forward-time Euler discrete method is used in the continuous-time model expressed in equation (11) in order to obtain the discrete model:

$$\begin{cases} i_d(k+1) = i_d(k) + T_s\left\{\alpha_d u_d(k) + \hat{F}_d(k)\right\} \\ i_q(k+1) = i_q(k) + T_s\left\{\alpha_q u_q(k) + \hat{F}_q(k)\right\} \end{cases} \tag{19}$$

Simplification of equation (15) gives

$$\begin{cases} u_d(k) = \dfrac{i_d(k+1) - i_d(k)}{T_s\alpha_d} - \dfrac{\hat{F}_d(k)}{\alpha_d} \\ u_q(k) = \dfrac{i_q(k+1) - i_q(k)}{T_s\alpha_q} - \dfrac{\hat{F}_q(k)}{\alpha_q} \end{cases} \tag{20}$$

To make the current track the expected current more accurately [32],

$$\begin{cases} i_d^* = i_d(k+1) \\ i_q^* = i_q(k+1) \end{cases} \tag{21}$$

Here, $i_d^* = 0$ is considered as the reference control, i_q^* is the q-axis current output of the speed outer loop, and $i_d(k)$ and $i_q(k)$ are the feedback outputs of the system at time k.

Therefore, the reference voltage of the system is obtained as

$$\begin{cases} u_d(k) = \dfrac{i_d^* - i_d(k)}{T_s\alpha_d} - \dfrac{\hat{F}_d(k)}{\alpha_d} \\ u_q(k) = \dfrac{i_q^* - i_q(k)}{T_s\alpha_q} - \dfrac{\hat{F}_q(k)}{\alpha_q} \end{cases} \tag{22}$$

III. CURRENT LIMIT CONTROL

Excessive current produces greater torque, which, in turn, affects the smooth operation of the motor and leads to a decrease in control performance. Therefore, a current-limiting link is designed. Equation (8) is discretized to obtain

$$\begin{cases} u_d(k) = \dfrac{L_0}{T_s} i_d(k+1) - (\dfrac{L_0}{T_s} - R_0) i_d(k) - L_0\omega_e i_q \\ u_q(k) = \dfrac{L_0}{T_s} i_q(k+1) - (\dfrac{L_0}{T_s} - R_0) i_q(k) \\ \quad + \omega_e(L_0 i_d + \psi_{f0}) \end{cases} \tag{23}$$

According to equation (19), when the dq-axis current is the highest at time $k+1$, the dq-axis voltage is also the highest at time k.

$$\begin{cases} u_{d(\max)} = \dfrac{L_0}{T_s} i_{d(\max)} - (\dfrac{L_0}{T_s} - R_0) i_d(k) - L_0\omega_e i_q \\ u_{d(\min)} = -\dfrac{L_0}{T_s} i_{d(\max)} - (\dfrac{L_0}{T_s} - R_0) i_d(k) - L_0\omega_e i_q \\ u_{q(\max)} = \dfrac{L_0}{T_s} i_{q(\max)} - (\dfrac{L_0}{T_s} - R_0) i_q(k) \\ \quad + \omega_e(L_0 i_d + \psi_{f0}) \\ u_{q(\min)} = -\dfrac{L_0}{T_s} i_{q(\max)} - (\dfrac{L_0}{T_s} - R_0) i_q(k) \\ \quad + \omega_e(L_0 i_d + \psi_{f0}) \end{cases} \tag{24}$$

Therefore, the maximum dq-axis current is set, and then, the amplitude of the dq-axis voltage is controlled to limit this maximum current to ensure that it lies within a reasonable interval. If we assume that the maximum values of the dq-axis current are $i_{d(\max)}$ and $i_{q(\max)}$, the amplitude of the dq-axis voltage can be expressed as equation (20).

Where $u_{d(\max)}$ and $u_{d(\min)}$ are the maximum and minimum values, respectively, of the d-axis voltage and $u_{q(\max)}$ and

$u_{q(\min)}$ are the maximum and minimum values, respectively, of the q-axis voltage.

The control structure of the MFPCC + NDC method proposed in this paper is shown in Fig (1).

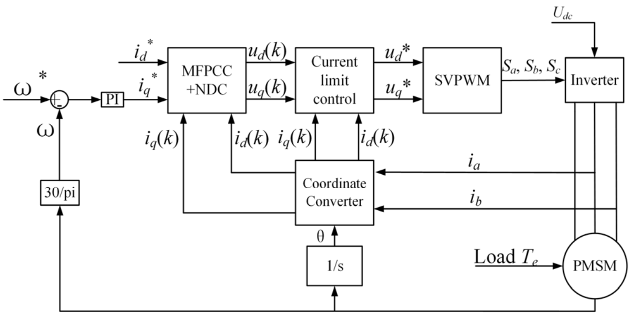

FIGURE 1. Control of PMSM system by MFPCC + NDC method.

IV. ANALYSIS OF SIMULATION RESULTS

To verify the effectiveness of the proposed method, simulation is performed using the MATLAB/Simulink platform. The simulation parameters are listed in Table 1.

TABLE 1. Simulation parameters.

Parameter	Value
Sampling period T_s	10 μs
Pole pairs p	4
Stator resistance R_0	0.958 Ω
Flux linkage Ψ_{f0}	0.1827 Wb
Inductance L_0	8.5 mH
Moment of inertia, J	0.003 kgm^2
DC-bus voltage U_{dc}	311 V
Variable 1, α	$[120, 120]^T$
Variable 2, l	$[1000, 1000]^T$

To examine the control performance of the model, the simulation is performed under two conditions and the rated speed of the motor is 1000 rad/s. Under one condition, the simulation is performed using precise parameters without any load. Under the other condition, the simulation is performed with variable parameters and an external load; under this latter condition, the parameters are varied; specifically, the inductance is varied to twice the original value and the flux linkage is varied to half the original value, and an external load (T_e) of 10 Nm is applied at $t = 0.2$ s.

To confirm the feasibility of the proposed MFPCC + NDC method, its performance is compared with those of the conventional PI control and the previously proposed MFPCC method [22] via simulations.

Figs 2(a)–(c) show the simulation results for the three methods, i.e., conventional PI control, MFPCC method, and proposed MFPCC + NDC method, respectively, under the condition of precise parameters and no load. Simulation results of four parameters, namely, speed, electromagnetic torque, d-axis current, and q-axis current, estimated by the three methods are selected for comparison. The simulation results reveal that the motor speed estimated by all three methods has a certain overshoot, but the overshoot in the value estimated by the conventional PI control is larger than those in the values estimated by the other two methods; additionally, the conventional PI control and MFPCC have large pulsations. However, our proposed MFPCC + NDC method provides stable speed operation and has a strong dynamic response, and it facilitates return of the motor speed to the rated speed in a relatively short time. For the parameter of electromagnetic torque, the MFPCC method has the largest pulsation, followed by conventional PI control; that is, the MFPCC + NDC method has the smallest pulsation. For the d-axis and q-axis currents, the conventional PI control has larger current ripple and a poorer tracking performance than the other two methods. The MFPCC + NDC method has smaller current ripple and better dynamic characteristics.

When the PMSM control system is subjected to parameter changes and unknown disturbances, both the control accuracy and the system performance decrease. To test the anti-interference performance and robustness of the model developed in this study, the PMSM inductance is doubled, the flux linkage is halved, and an external load (T_e) of 10 Nm is applied at $t = 0.2$ s.

Fig 3 shows the simulation results under this condition of variable parameters and interference in the form of an external load. In the case of the motor speed, the conventional PI control has a larger overshoot and significantly larger speed ripple than the other two methods. Although the MFPCC and MFPCC + NDC methods both have certain overshoots, the latter method is able to rapidly track the motor speed to the rated speed and provide stable speed operation almost without any pulsation. In the case of the electromagnetic torque, the conventional PI control and the MFPCC method both have large torque ripple, which is unconducive to the smooth operation of the motor; in contrast, the MFPCC + NDC method has smaller torque ripple, because of which it can perform rapid tracking and maintain stable operation when an external load is applied. In the case of the d-axis and q-axis currents, the conventional PI control and MFPCC both clearly have large current ripple and poor current tracking performances. The conventional PI control d-axis current has been in a state of large fluctuations, and when 0.2s is added to the load, the d-axis current cannot accurately track the rated current, and the control accuracy is the lowest. In the estimation of the d-axis current by the MFPCC method under application of an external load, the current ripple is noticeably larger and the jitter is also worse. The MFPCC + NDC method has high anti-interference performance and high robustness under the condition of variable parameters and an external load. This

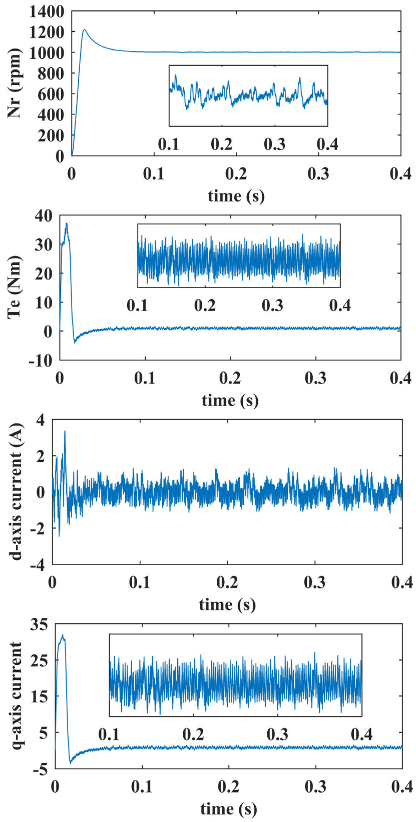

(a) Speed, electromagnetic torque, *d*-axis current, and *q*-axis current estimated by conventional PI control

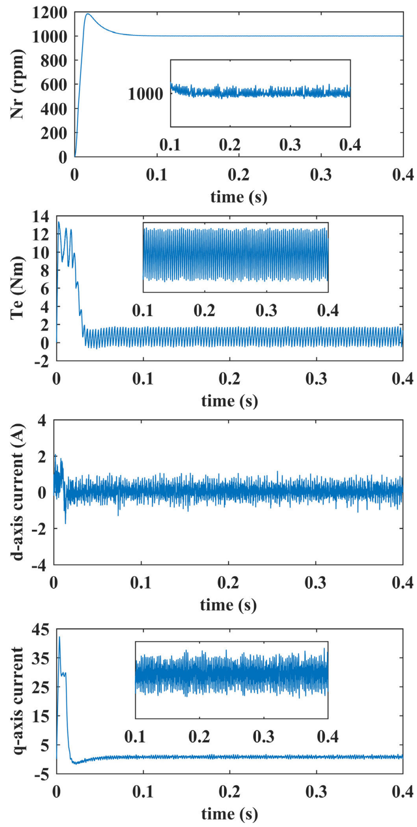

(b) Speed, electromagnetic torque, *d*-axis current, and *q*-axis current estimated by previously proposed MFPCC method

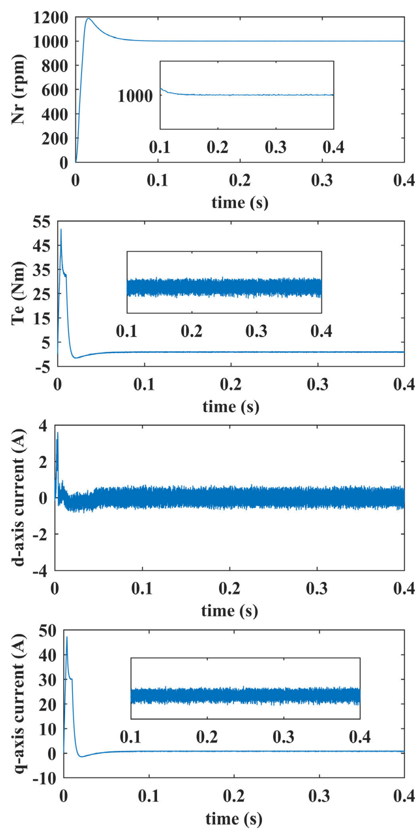

(c) Speed, electromagnetic torque, *d*-axis current, and *q*-axis current estimated by MFPCC + NDC method proposed in present study

FIGURE 2. Simulation results under condition of precise parameters and no load: (a) conventional PI control, (b) MFPCC method, and (c) MFPCC + NDC method.

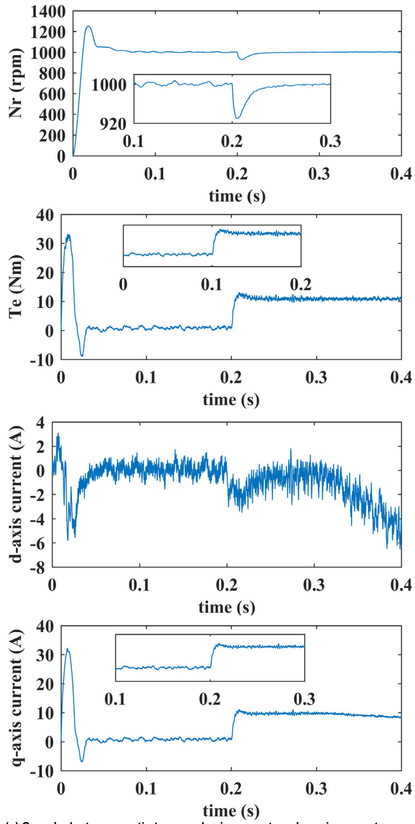

(a) Speed, electromagnetic torque, *d*-axis current, and *q*-axis current estimated by conventional PI control

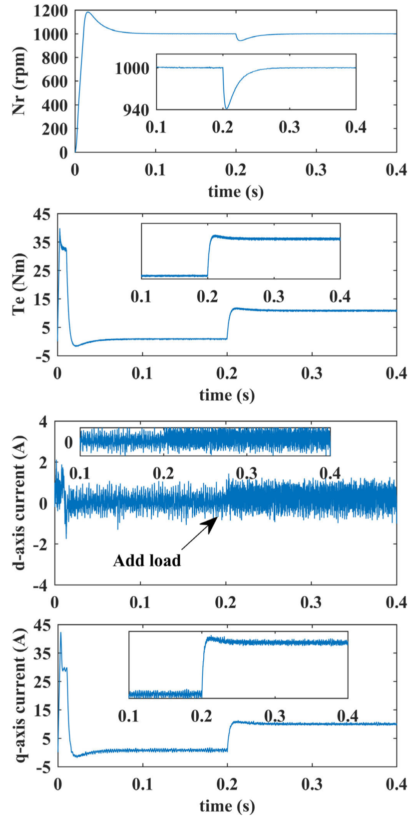

(b) Speed, electromagnetic torque, *d*-axis current, and *q*-axis current estimated by previously proposed MFPCC method

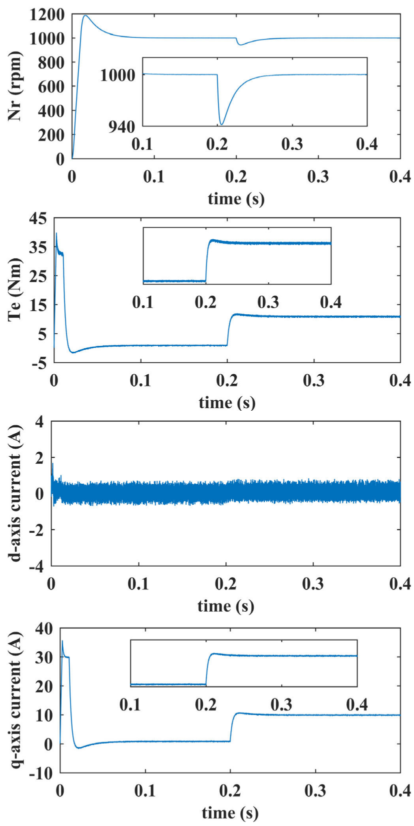

(c) Speed, electromagnetic torque, *d*-axis current, and *q*-axis current estimated by MFPCC + NDC method proposed in present study

FIGURE 3. **Simulation results under condition of variable parameters and external load: (a) conventional PI control, (b) MFPCC method, and (c) MFPCC + NDC method.**

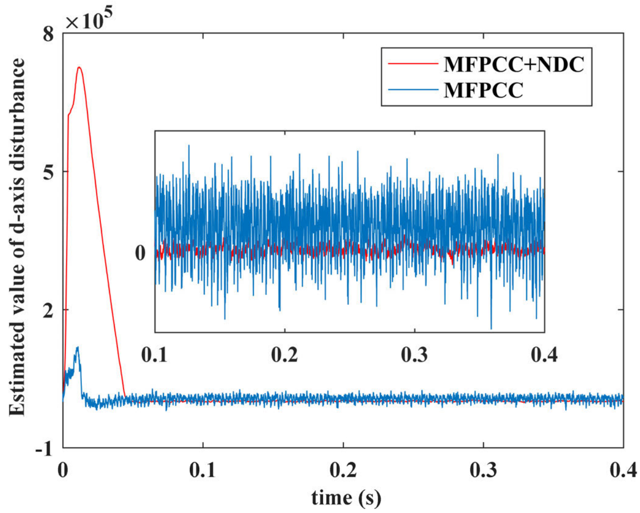

(a) Estimation of total disturbance of *d*-axis system

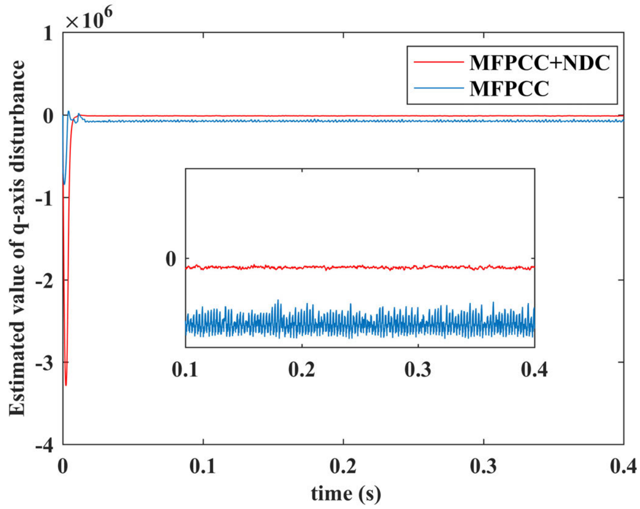

(b) Estimation of total disturbance of *q*-axis system

FIGURE 4. **Comparison of simulation results obtained using MFPCC and MFPCC + NDC methods under condition of precise parameters and no load: (a) estimation of total disturbance of *d*-axis system and (b) estimation of total disturbance of *q*-axis system.**

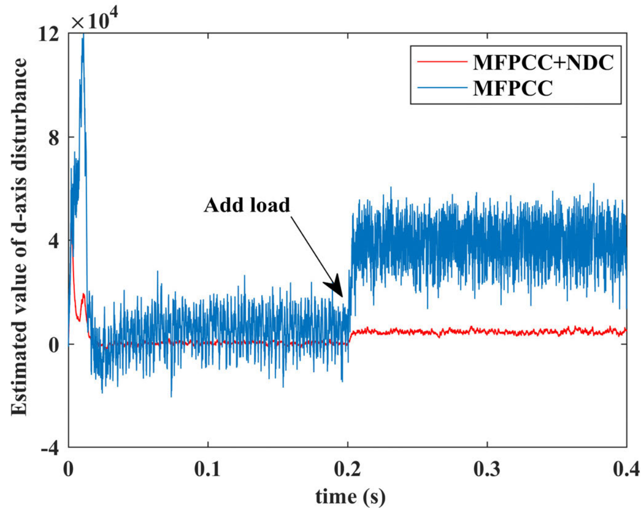

(a) Estimation of total disturbance of *d*-axis system

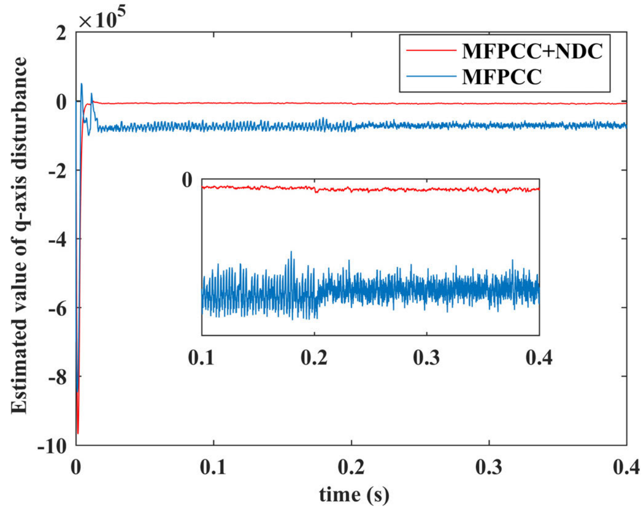

(b) Estimation of total disturbance of *q*-axis system

FIGURE 5. **Comparison of simulation results obtained using MFPCC and MFPCC + NDC methods under condition of variable parameters and external load: (a) estimation of total disturbance of *d*-axis system and (b) estimation of total disturbance of *q*-axis system.**

method has an ideal tracking performance and better dynamic characteristics, and it does not generate large speed, torque, or current ripple.

To test the effectiveness of the proposed method and verify the estimated accuracy and stability of the total disturbance of the system, the MFPCC and MFPCC + NDC methods are compared in terms of the total disturbance of the *dq*-axis system. The comparison is performed under two conditions: (1) precise parameters and no load and (2) variable parameters and an external load.

Fig 4 shows a comparison of the total disturbance of the *dq*-axis system estimated by the MFPCC and MFPCC + NDC methods under the condition of precise parameters and no load. The results show that the MFPCC method estimates the total disturbances of the *d*-axis and *q*-axis systems with larger pulsation, more obvious chattering, and lower accuracy (especially in the case of the *q*-axis system). In contrast, the MFPCC + NDC method estimates the total disturbance of the system with high accuracy and good stability and without any obvious pulsation. The total disturbance of the *d*-axis system estimated by the proposed method has a large overshoot initially; however, it rapidly drops to the normal value, and the method has a faster dynamic response and better dynamic characteristics.

Fig 5 shows a comparison of the total disturbance of the *dq*-axis system estimated by the MFPCC and MFPCC + NDC methods under the condition of variable parameters and an external load. The results reveal that when the parameters are changed and an external load is applied, the MFPCC method estimates the total disturbance of the system with more obvious chattering, larger pulsation, significantly lower accuracy, and poorer stability. When an external load is applied in the estimation of the total disturbance of the d-axis system, the model will encounter external interference and the estimated value of the total disturbance of the d-axis system will suddenly change.; therefore, the total disturbance cannot be estimated accurately. The MFPCC + NDC method, however, provides an accurate and stable estimate of the total system disturbance when the system is subjected to parameter changes and external load disturbances, and it does so without any obvious pulsation and chattering and has high anti-interference performance and high robustness.

From Fig 2 to Fig 5, under precise parameters and no-load conditions, the MFPCC+NDC method can smoothly track the *dq*-axis rated current without generating large current ripple, the motor runs smoothly, and the estimation of the total disturbance of the system is relatively accurate and stable, the output ripple of the system is small and the tracking performance is better. Under the condition of variable parameters and an external load, the conventional PI control method and MFPCC method have obvious chattering, large output ripple, and poor tracking performance. Under this condition, the total disturbance estimated by the MFPCC method has an obvious deviation, with obvious overshoots and severe chattering. However, The MPCPC+NDC method can still track the rated current and speed smoothly, and estimate the total disturbance of the system more accurately and stably.

V. CONCLUSION

With the aim of resolving the problem of model mismatch caused by parameter changes and unknown disturbances, which leads to a decrease in control performance, this paper proposes an ultra-local model-free predictive current control method based on nonlinear disturbance compensation (MFPCC + NDC). Simulation results show that under two conditions the MFPCC + NDC method is able to estimate the total disturbance of the system more accurately and stably; furthermore, the method provides a stable system output and its tracking performance and dynamic characteristics are better than those of the other two methods. All these results demonstrate that the proposed MFPCC + NDC method has high anti-interference performance and high robustness against disturbances.

DATA AVAILABILITY

The data used to support the findings of this study are included within the article.

CONFLICTS OF INTEREST

The authors declare that they have no conflicts of interest.

REFERENCES

[1] J. Yu, P. Shi, and L. Zhao, "Finite-time command filtered backstepping contranti-interference performanceol for a class of nonlinear systems," *Automatica*, vol. 92, pp. 173–180, Jun. 2018.

[2] F. Ban, G. Lian, J. Zhang, B. Chen, and G. Gu, "Study on a novel predictive torque control strategy based on the finite control set for PMSM," *IEEE Trans. Appl. Supercond.*, vol. 29, no. 2, Mar. 2019, Art. no. 3601206.

[3] W. Xu, A. K. Junejo, Y. Liu, and M. R. Islam, "Improved continuous fast terminal sliding mode control with extended state observer for speed regulation of PMSM drive system," *IEEE Trans. Veh. Technol.*, vol. 68, no. 11, pp. 10465–10476, Nov. 2019.

[4] Y. Wang, Y. Xu, and J. Zou, "Sliding-mode sensorless control of PMSM with inverter nonlinearity compensation," *IEEE Trans. Power Electron.*, vol. 34, no. 10, pp. 10206–10220, Oct. 2019.

[5] H. Fan and Y. C. Wang, "Research on the characteristics of PMSM vector control system based on speed sliding mode controller," *Appl. Mech. Mater.*, vols. 130–134, pp. 1142–1147, Oct. 2011.

[6] J.-W. Jung, V. Quoc Leu, T. Duc Do, E.-K. Kim, and H. Ho Choi, "Adaptive PID speed control design for permanent magnet synchronous motor drives," *IEEE Trans. Power Electron.*, vol. 30, no. 2, pp. 900–908, Feb. 2015.

[7] J. Liu, M.-Z. Huang, and Y. Wang, "Research on vector-control system of PMSM based on internal model control of current loop," in *Proc. 2nd Int. Workshop Comput. Sci. Eng.*, Oct. 2009, pp. 297–301.

[8] K. Liu, C. Hou, and W. Hua, "A novel inertia identification method and its application in PI controllers of PMSM drives," *IEEE Access*, vol. 7, pp. 13445–13454, 2019.

[9] C. Xia, J. Zhao, Y. Yan, and T. Shi, "A novel direct torque and flux control method of matrix converter-fed PMSM drives," *IEEE Trans. Power Electron.*, vol. 29, no. 10, pp. 5417–5430, Oct. 2014.

[10] M. H. Vafaie, B. Mirzaeian Dehkordi, P. Moallem, and A. Kiyoumarsi, "A new predictive direct torque control method for improving both steady-state and transient-state operations of the PMSM," *IEEE Trans. Power Electron.*, vol. 31, no. 5, pp. 3738–3753, May 2016.

[11] M. H. Vafaie, B. M. Dehkordi, P. Moallem, and A. Kiyoumarsi, "Improving the steady-state and transient-state performances of PMSM through an advanced deadbeat direct torque and flux control system," *IEEE Trans. Power Electron.*, vol. 32, no. 4, pp. 2964–2975, Apr. 2017.

[12] L. A. Adase, I. M. Alsofyani, and K.-B. Lee, "Predictive torque control with simple duty-ratio regulator of PMSM for minimizing torque and flux ripples," *IEEE Access*, vol. 8, pp. 2373–2381, 2020.

[13] S. Ding and S. Li, "Second-order sliding mode controller design subject to mismatched term," *Automatica*, vol. 77, pp. 388–392, Mar. 2017.

[14] L. Liu, W. X. Zheng, and S. Ding, "An adaptive SOSM controller design by using a Sliding-Mode-Based filter and its application to buck converter," *IEEE Trans. Circuits Syst. I, Reg. Papers*, vol. 67, no. 7, pp. 2409–2418, Jul. 2020.

[15] Q. Liu and K. Hameyer, "Torque ripple minimization for direct torque control of PMSM with modified FCSMPC," *IEEE Trans. Ind. Appl.*, vol. 52, no. 6, pp. 4855–4864, Nov. 2016.

[16] S. Chai, L. Wang, and E. Rogers, "A cascade MPC control structure for a PMSM with speed ripple minimization," *IEEE Trans. Ind. Electron.*, vol. 60, no. 8, pp. 2978–2987, Aug. 2013.

[17] X. Zhang, L. Zhang, and Y. Zhang, "Model predictive current control for PMSM drives with parameter robustness improvement," *IEEE Trans. Power Electron.*, vol. 34, no. 2, pp. 1645–1657, Feb. 2019.

[18] H. Liu and S. Li, "Speed control for PMSM servo system using predictive functional control and extended state observer," *IEEE Trans. Ind. Electron.*, vol. 59, no. 2, pp. 1171–1183, Feb. 2012.

[19] X. Liu, C. Zhang, K. Li, and Q. Zhang, "Robust current control-based generalized predictive control with sliding mode disturbance compensation for PMSM drives," *ISA Trans.*, vol. 71, pp. 542–552, Nov. 2017.

[20] X. Sun, M. Wu, G. Lei, Y. Guo, and J. Zhu, "An improved model predictive current control for PMSM drives based on current track circle," *IEEE Trans. Ind. Electron.*, early access, Apr. 13, 2020, doi: 10.1109/TIE.2020.2984433.

[21] Y. Zhou, H. Li, and H. Zhang, "Model-free deadbeat predictive current control of a surface-mounted permanent magnet synchronous motor drive system," *J. Power Electron.*, vol. 14, pp. 265–274, Jan. 2019.

[22] C.-K. Lin, T.-H. Liu, J.-T. Yu, L.-C. Fu, and C.-F. Hsiao, "Model-free predictive current control for interior permanent-magnet synchronous motor drives based on current difference detection technique," *IEEE Trans. Ind. Electron.*, vol. 61, no. 2, pp. 667–681, Feb. 2014.

[23] M. Fliess, and C. Join, "Model-free control," *Int. J. Control*, vol. 86, no. 12, pp. 2228–2252, 2013.

[24] Y. Zhou, H. Li, and H. Yao, "Model-free control of surface mounted PMSM drive system," in *Proc. IEEE Int. Conf. Ind. Technol. (ICIT)*, Mar. 2016, pp. 175–180.

[25] Y. Zhang, J. Jin, and L. Huang, "Model-free predictive current control of PMSM drives based on extended state observer using ultra-local model," *IEEE Trans. Ind. Electron.*, early access, Feb. 5, 2020, doi: 10.1109/TIE.2020.2970660.

[26] J. Yang, S. Li, and X. Yu, "Sliding-mode control for systems with mismatched uncertainties via a disturbance observer," *IEEE Trans. Ind. Electron.*, vol. 60, no. 1, pp. 160–169, Jan. 2013.

[27] Y. Zhou, H. Li, and H. Zhang, "Model-free deadbeat predictive current control of a surface-mounted permanent magnet synchronous motor drive system," *J. Power Electron.*, vol. 18, no. 1, pp. 103–115, Jan. 2018.

[28] X.-H. Chang, Y. Liu, and M. Shen, "Resilient control design for lateral motion regulation of intelligent vehicle," *IEEE/ASME Trans. Mechatronics*, vol. 24, no. 6, pp. 2488–2497, Dec. 2019.

[29] Z.-M. Li, X.-H. Chang, and J. H. Park, "Quantized static output feedback fuzzy tracking control for discrete-time nonlinear networked systems with asynchronous event-triggered constraints," *IEEE Trans. Syst., Man, Cybern. Syst.*, early access, Aug. 15, 2019, doi: 10.1109/TSMC.2019.2931530.

[30] S. Ding, W.-H. Chen, K. Mei, and D. J. Murray-Smith, "Disturbance observer design for nonlinear systems represented by input–output models," *IEEE Trans. Ind. Electron.*, vol. 67, no. 2, pp. 1222–1232, Feb. 2020.

[31] X. Liu, H. Yu, J. Yu, and L. Zhao, "Combined speed and current terminal sliding mode control with nonlinear disturbance observer for PMSM drive," *IEEE Access*, vol. 6, pp. 29594–29601, 2018.

[32] Y. Zhang, D. Xu, and L. Huang, "Generalized Multiple-Vector-Based model predictive control for PMSM drives," *IEEE Trans. Ind. Electron.*, vol. 65, no. 12, pp. 9356–9366, Dec. 2018.

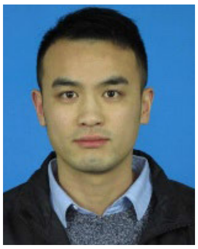

LINGLIANG XU received the bachelor's degree in mechanical engineering from the Hefei University of Technology, in 2018. He is currently pursuing the degree (direct) in weapon science and technology with the Xi'an Research Institute of High-Tech, Xi'an, China, mainly engaged in the use and support of weapon systems.

GUIMING CHEN received the bachelor's and master's degrees in mechanical engineering and the Ph.D. degree in weapon science and technology from the Xi'an Research Institute of High-Tech, Xi'an, China, in 1988, 1991, and 2004, respectively. He is currently a Professor with the Combat Support College, Xi'an Research Institute of High-Tech, mainly engaged in weapon and equipment management.

QIAOYANG LI received the bachelor's degree in electronic engineering from the Xi'an Research Institute of High-Tech, in 2019, where he is currently pursuing the master's degree in management science and engineering, mainly engaged in national defense engineering and project management.